Nedis-Serpent simulation of a neutron source assembly with complex internal heterogeneous structure

Sergey V. Bedenko[1*], Gennady N. Vlaskin[2], Nima Ghal-Eh[3,4], Igor O. Lutsik[1], Ruslan Irkimbekov[5], Faezeh Rahmani[6] & Hector Rene Vega-Carrillo[7]

[1]School of Nuclear Science and Engineering, Tomsk Polytechnic University, Tomsk, Russia

[2]Innovation Technology Centre for the PRORYV Project, ROSATOM, Moscow, Russia

[3]School of Physics, Damghan University, Damghan, Iran

[4]Department of Physics, Faculty of Sciences, Ferdowsi University of Mashhad, Mashhad, Iran

[5]National Nuclear Center of the Republic of Kazakhstan, Kurchatov, Kazakhstan

[6]Department of Physics, K. N. Toosi University of Technology, Tehran, Iran

[7]Academic Unit of Nuclear Studies of the Autonomous University of Zacatecas
Zacatecas, Zac., Mexico

Abstract

The hybrid use of Nedis-2m and Serpent 2.1.30 codes to predict the radiation characteristics (*i.e.*, neutron yield and energy spectrum) of an Am-Be source with a fine-grained mixture of americium dioxide (AmO_2) and beryllium (Be) core was studied with a focus on the grain size influence on the simulation results. The study showed that the fine-grained structure of the source core would decrease the number of alpha particles participating in the nuclear reactions with $^{17,18}O$ and ^{9}Be nuclei, which softened the neutron energy spectrum and reduced the neutron yield. The simulations also confirmed that the source core made of the stable crystals of $AmBe_{13}$ intermetallic alloy would improve the neutron yield to maximum 50% compared to the core made of AmO_2. Moreover, a source with a variable neutron yield was proposed with a heterogeneous core of AmO_2 rods embedded in Be. The neutron energy spectrum of heterogeneous source resembled the energy spectrum of Deuterium-Tritium (DT) neutrons which were generated in a long magnetic trap with high-temperature plasma. The subcritical irradiation facility assembled from the n^{th} number of heterogeneous Am-Be source can be used to study the properties of materials and the equipment operating in the epithermal and fast neutron spectra. The use of a heterogeneous ^{241}Am-Be assembly, as a basic element of an irradiation installation, simplifies the handling and operation procedures because it is easily disabled by removing the Be layer, or by inserting a sheet of the appropriate size and material between the Be and Am rod.

Keywords: Radioisotopic neutron sources; (α,n)-reaction; heterogeneous structure; Nedis-2m; Serpent 2.1.30.

1.- INTRODUCTION

Radioisotope neutron sources are still widely used in various industrial installations (Asamoah *et al*., 2011; Yücel *et al*., 2014; Didi *et al*., 2016; Balaghi *et al*., 2018), constructed either based on a fine-grained mixture of Pu and Be dioxide, mixtures of $Am/AmO_2/Am_2O_3$ and Be oxides, or based on pure intermetallic alloys Pu-Be and Am-Be (Geiger and Van Der Zwan, 1975; Croft, 1989). In different experimental studies, such as neutron activation analysis, applied nuclear physics and medicine, it is important to have a compact and a mobile encapsulated neutron source, preferably without Pu. Such radioisotope sources are made by mixing or fusing heavy elements (*e.g.*, Po, Ra, Am, Cf) with low atomic weight elements, based on (α,n) and spontaneous fission reactions in light and heavy nuclei, respectively. Notes should be taken that the source neutrons are always accompanied by gamma rays, however, with lower emission probability (Vega-Carrillo *et al*., 2002; Vitorelli *et al*., 2005; Liu *et al*., 2007).

Am-Be sources are more frequently used than others, which is due to the long half-life of ^{241}Am ($T_{1/2}$ = 432.6 y), almost stable and fixed neutron yield. Such radioisotope sources are compact and - in most cases - mobile capsules with no need to very large neutron/gamma shields (Vega-Carrillo and Martinez-Ovalle, 2016).

Am-Be sources normally have their own characteristic neutron energy spectrum (Kluge and Weise, 1982; Marsh *et al.*, 1995; Lorch 1973; Lebreton *et al*., 2007), which may vary depending on the capsule design, its composition, the presence of light- and medium-weight impurity elements, and the grain size/distribution of the mixed components in the active part of the source (*i.e.*, the source core) (Van Der Zwan 1968; Marsh *et al*., 1995; Tsujimura and Yoshida, 2007, Vlaskin and Khomiakov, 2017; Griesheimer *et al*., 2017).

In many applications of Am-Be neutron source, either the ISO-recommended (ISO 8529-1, 2001) or the measurement data (Kluge and Weise, 1982; Marsh *et al*., 1995; Lorch 1973) of normalized neutron energy spectrum (*i.e.*, dN_n/dE_n) can be used, where the integral neutron

yield, $Q_n(E_\alpha) = \sum I_{\alpha i}(E_{\alpha i}) \times Y_{ni}(E_{\alpha i})$, in such applications is usually known or, if necessary, it can be calculated.

Assuming that the mixed components form a molecular compound, this calculation can be based on alpha-decay data ($I_{\alpha i}$ [particles], y(i) [Bq × s]$^{-1}$) of the heavy isotopes as well as available and highly accurate experimental and/or calculated neutron yield data Y_{ni} (n/s per α particle). Further tracking of generated neutrons through (α,n) and fission processes normally requires a Monte Carlo neutron transport code.

Several high-precision data on the yield analysis of neutrons generated via α-decay of actinides, subsequent (α,n) reactions to the light target elements, and their binary compounds can be found in the literature (Bair and Gomez del Campo, 1979; West and Sherwood, 1982; Heaton *et al*., 1989; Murata and Shibata, 2002; Murata *et al*., 2006; Vlaskin *et al*., 2015; Simakov and Berg, 2017). As an example, the measured values of the neutron yield of (α,n) reaction on light elements and binary compounds in a wide energy range of alpha particles are presented in (Bair and Gomez del Campo, 1979; West and Sherwood, 1982). Likewise, an interesting study has been devoted to high-precision measurements of neutron yield with a measurement error of less than 2%, for alpha particle energies ranging from 3.6 to 10 MeV (West and Sherwood, 1982).

The measurements reported in (Heaton *et al*., 1989) are also with the neutron yield of (α,n) reaction, for alpha particle energies within the range of 1 to 9.8 MeV. A modern analysis of high-precision measurement and calculation data on neutron yields is available in (Murata *et al*., 2006; Vlaskin *et al*., 2015; Simakov and Berg, 2017), too. The data published in (Simakov and Berg, 2017) may be considered as the update of previous reference tables published by Los Alamos National Laboratory (LANL) in 1991 (Reilly *et al*., 1991). In (Vlaskin *et al*., 2015), authors have made neutron yield calculations based on their own evaluation of (α,n) cross-sections as well as the evaluated data published by LANL (Wilson *et al*., 1984) and Japan Atomic Energy Research Institute (JENDL/AN-2005) (Murata *et al*., 2006).

In the studies undertaken by Nedis-2m group (Vlaskin, 2006; Vlaskin and Khomiakov, 2017), the exact $Y_{ni}(E_{\alpha i})$ values for light elements, from Li to K, have been calculated for the alpha particle energy range of 4 to 9 MeV. The Nedis-2m benchmarks confirmed that the largest discrepancy between calculated $Y_{ni}(E_{\alpha i})$ values and measurement data for the alpha energy range of 4.2 to 4.3 MeV available in (West and Sherwood, 1982), does not exceed ~ 5%, whilst the discrepancy between the Nedis-2m data based on LANL and JENDL/AN-2005 evaluations, remains below ~ 5.5%. Nedis-2m data, calculated based on JENDL/AN-2005, do not diverge from the measurement data (West and Sherwood, 1982) by values less than 1.5% in the alpha particle energy range of 4.1 to 8 MeV. It is noteworthy that the error of Nedis-2m calculation data for (α,n) reaction on Be is normally less than 3%, regardless of the cross-section data library (Vlaskin, 2006).

The approach described above is relatively simple and practically attractive from time consumption point of view, as it gives $Q_n(E_\alpha)$ values with acceptable accuracy (up to ~ 30%) as well as the neutron energy spectrum, dN_n/dE_n, without using computational codes. It should be noted that in modeling ($Am/AmO_2/Am_2O_3$)-Be source based on a fine-grained mixture, one can use the above approach by considering the active part (*i.e.*, source core) of the capsule as a molecular compound of homogeneous mixture. Moreover, for a perfect mixing of the components where the grain size of Am oxide crystals remains less than 2 μm, the transverse grain size (d_{grain}) should be much less than the mean free path of alpha particles (r_α) in AmO_2, which itself causes the emitted alpha particles from the grain to become completely stopped in Be region.

In most Am-Be neutron sources, the core density after mechanical mixing and subsequent pressing is less than 1.5g/cm^3 (Liu *et al*., 2007; Tsujimura *et al*., 2007). In other words, the above approach for the grain sizes greater than 3 μm results in an overestimated data. This might be useful in, for example, stationary biological protection or in the development of handling procedures necessary for the manufacture, maintenance and disposal of a neutron source.

A thorough review of the use of neutron sources in neutron activation analysis for monitoring and control of nuclear materials and related topics is given in (Vega-Carrillo and Martinez-Ovalle, 2016; Vlaskin *et al*., 2015; Plevaka *et al*., 2015; Bedenko *et al*., 2019), where a more accurate (<10%) neutron yield value and its energy spectrum are necessary.

The exact values of the neutron yield, $Q_n(E_\alpha)$, and energy spectrum, dN_n/dE_n, can be calculated by using the following programs: Nedis-2m (Vlaskin, 2006), Origen-S (Hermann and Westfall, 1995), SOURCES-4C (Wilson *et al*., 2002), USD (Mei *et al*., 2009; Fernandes *et al*., 2017), CHARS (Leniau and Wilson, 2014), MC21 (Griesheimer *et al*., 2017). These programs mainly focus on the neutron yield and energy spectrum calculations, however, it is necessary for the current status of some programs to undertake a careful justification and/or modification for the capsule cores of complex heterogeneous structure. Examples of such modifications can be found in (Bedenko *et al*., 2019; Ghal-Eh *et al*., 2019; Dim and Aghara, 2019). In (Ghal-Eh *et al*., 2019), a methodology has been proposed based on an analytical model for the calculation of the neutron yield and the energy spectrum of the heterogeneous Am-Be source using SOURCES-4C and MCNPX codes, where the source core consisted of americium and americium oxide rods ($Am/AmO_2/Am_2O_3$) surrounded by metal Be.

The proposed heterogeneous geometry can provide a neutron source with a variable neutron yield, easy-to-shut down and easy-to-waste process features (Ghal-Eh *et al*., 2019). The SOURCES-4C is a reference and world-famous code, which is distributed by the Nuclear Energy Agency at (https://oecd-nea.org/). SOURCES-4C is not suitable for all calculation purposes.

The Nedis-2m is thought to be more efficient than SOURCES-4C in some applications such as neutron activation analysis, modern nuclear physics studies and medicine.

Nedis-2m is capable to calculate the production rate and continuous energy spectra of neutrons generated via (α,n) reaction on Li, Be, B, C, O, F, Ne, Na Mg, Al, Si, P, S, Cl, Ar,

and K. Nedis-2m takes into account the anisotropic angular distribution of neutrons of (α,n) reaction in center-of-mass system within the alpha emitting source material. It also calculates the spontaneous fission spectra with evaluated half-life, spontaneous fission branching, ν-averaged per fission, and Watt spectrum parameters.

The Nedis-2m results can be used basically as the input to a Monte Carlo code for full simulation purposes. Nedis-2m is successful in reproducing the spectrum structures due to its evaluated cross-sections for various excited states of the residual nuclei, as well as the anisotropic angular emission in the center-of-mass system, particularly for ^{7}Li, ^{9}Be and ^{13}C.

In this study, the neutron yield and energy spectrum of the widely-used Amersham X.14 radioisotopic source based on a fine-grained mixture of AmO_2 and Be have been examined. In addition, the possibility of producing the maximum neutron yield of chemically-stable Am crystals and intermetallic compounds has been investigated.

Based on a recent methodology introduced by Ghal-Eh *et al*., (2019), the well-known simulation codes of Nedis-2m and Serpent 2.1.30 (Leppänen *et al*., 2015) have been used to propose a procedure for neutron yield and energy spectrum calculations of a heterogeneous radioisotopic neutron source. Moreover, a comparative analysis of both integral and spectral characteristics of the above-mentioned neutron source has been carried out.

The possibility of using the proposed calculation methodology for studying the neutronic and radiation characteristics of subcritical breeding media of a complex heterogeneous structure has been described, too.

2.- MATERIALS AND METHODS

2.1.-Nedis-2m simulation of AmO_2-Be neutron source

The widely-used Amersham X.14 capsule has been selected in the present study (Amersham/Searle, 1976), to simulate the neutron component of radiation characteristics,

In Figure 1 is shown the model of the neutron source. The Amersham X.14 capsule has a complex heterogeneous structure with a fine-grained mixture of AmO_2 and Be crystals ($d_{grain} \leq r_\alpha$). The grain size and density of the mixed components in this type of capsules may normally vary from 1 to 10 μm (Van Der Zwan, 1968) and from 0.9 to 1.5 g/cm^3 (Griesheimer *et al*., 2017; Liu *et al*., 2007), respectively.

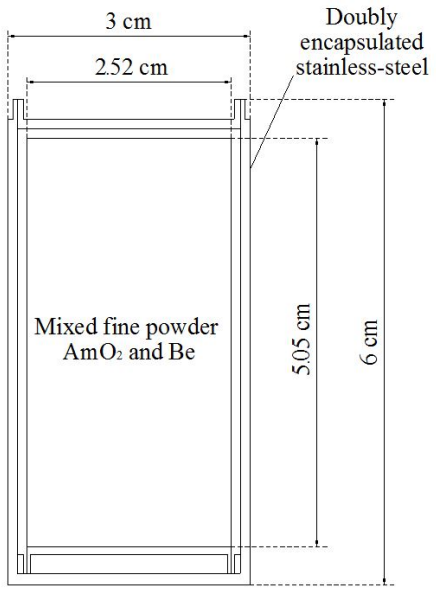

Figure 1.- The 3D model of the AmO_2-Be source used in the calculations.

Since the details of material composition and its internal structure of X.14 capsule are commercial secrets of the manufacturer (Amersham International plc), it has been assumed that the AmO_2-Be source is a mixture of grained powder of AmO_2 (ρ = 10.58 g/cm^3) and a metallic Be (ρ = 1.85 g/cm^3) in proportions of 1:12 which was pressed to the density of 1.5 g/cm^3.

Conventionally, the AmO_2 grain size is assumed to be 8 μm (Liu *et al*., 2007). The composition of the homogenized mixture of the AmO_2-Be source used in the calculations is listed in Table 1. The capsule shell material is stainless steel (Amersham/Searle, 1976), with the following composition (% wt): C (0.004), Mn (1.59), P (0.011), S (0.008), Si (0.37), Cr (16.96), Ni (13.61), Mo (2.29), Fe (65.16).

It has been assumed in the simulations that the alpha particles emitted from the AmO_2 grain either stop in Be or return to the AmO_2 grain and stop there. In this study, the Nedis-2m simulations of neutron energy spectrum, represented in Fig. 2 (lines (1) - (4)) and Fig. 3, show promising agreement with both the SOURCES-4C calculations (Fig. 2, line (5)) and the measurements (Kluge and Weise, 1982) (Fig. 3). The differences in spectra (1) and (5) (Fig. 2) can be attributed to the anisotropy of neutron emission in the center of mass of (α,n) reaction included in Nedis-2m.

Table 1.- Composition of AmO_2-Be source core.

Nuclide	Nuclide density [nuclides/(b·cm)]	Isotopic abundance [%]	Nuclide atomic fraction	Nuclide mass fraction	Mass [g]
^{9}Be	9.265E-02	100.000	9.918E-01	9.231E-01	34.875
^{16}O	5.078E-04	99.757	5.481E-03	8.995E-03	0.341
^{17}O	1.934E-07	0.0380	2.088E-06	3.426E-06	
^{18}O	1.044E-06	0.2050	1.126E-05	1.848E-05	
^{241}Am	2.408E-04	94.613	2.599E-03	6.425E-02	2.520
^{242}Am	9.153E-06	3.5960	9.879E-05	2.442E-03	
^{243}Am	4.558E-06	1.7910	4.920E-05	3.341E-06	

To verify the Nedis-2m code simulations, a test calculation has been performed on a 37 GBq ^{241}Am-Be source (Amersham X.3 capsule) of different AmO_2 grain diameters, where the grain density, the mass of AmO_2 core and, the Be mass were 11.7 g/cm^3, 0.37 g and 4.6 g, respectively. The configuration, composition and internal structure of the capsule has been taken from (Lorch, 1973).

The simulation results illustrated in Fig. 4 and listed in Table 2 show a good agreement (± 5%) between the calculation data of the present work and the study published in [Tsujimura and Yoshida, 2007].

The fine-grained structure of the capsule core normally leads to a decrease in the integral neutron yield (see Fig. 2, Table 2), however, the neutron yield can increase by using the stable crystal of an intermetallic compound $AmBe_{13}$ (Van Der Zwan, 1968).

Fig. 5 represents the simulation results for the Amersham X.14 capsule, with a mixture of $AmBe_{13}$ grained powder (ρ = 3.71 g/cm^3) and metal Be (ρ = 1.85 g/cm^3) as an active part. The density of the mixture in the active part is 1.5 g/cm^3 whilst the mixing ratio of the components is 1:12, which is identical to AmO_2-Be source.

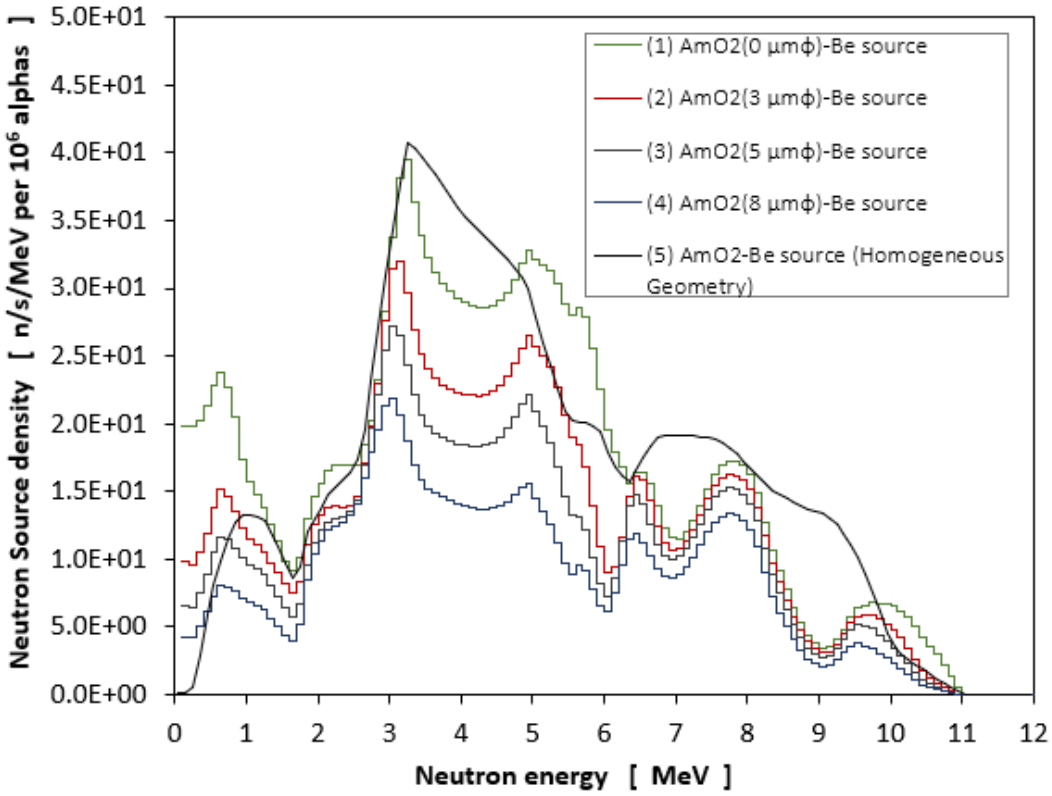

Figure 2.- Comparison between energy spectrum of neutrons produced in AmO_2 in Nedis-2m (the current study) and SOURCES-4C (homogeneous geometry) simulations.

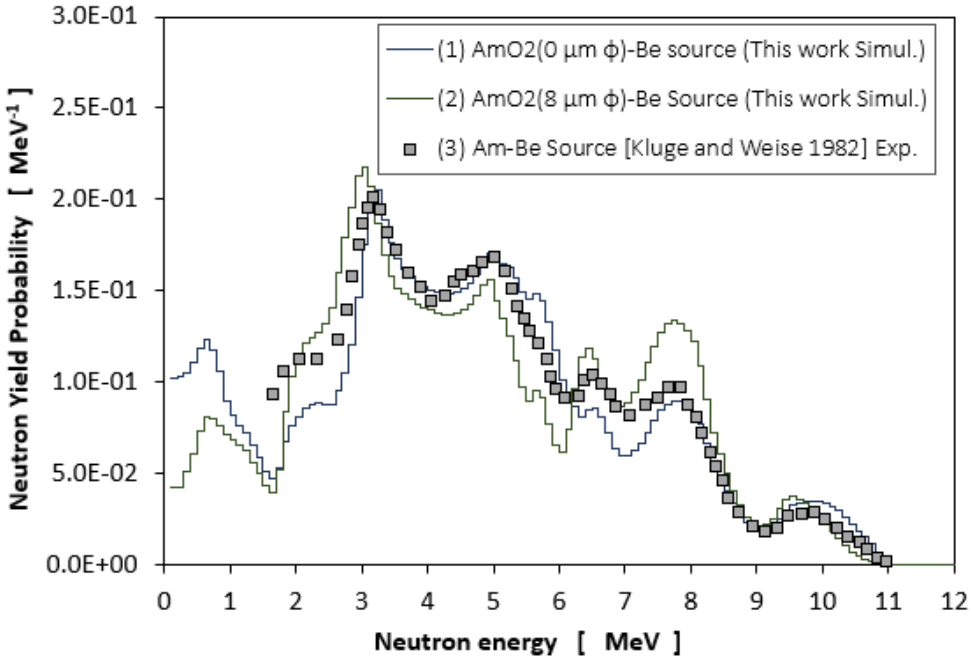

Figure 3.- Normalized neutron energy spectrum: comparison between Nedis-2m simulations and measurement data.

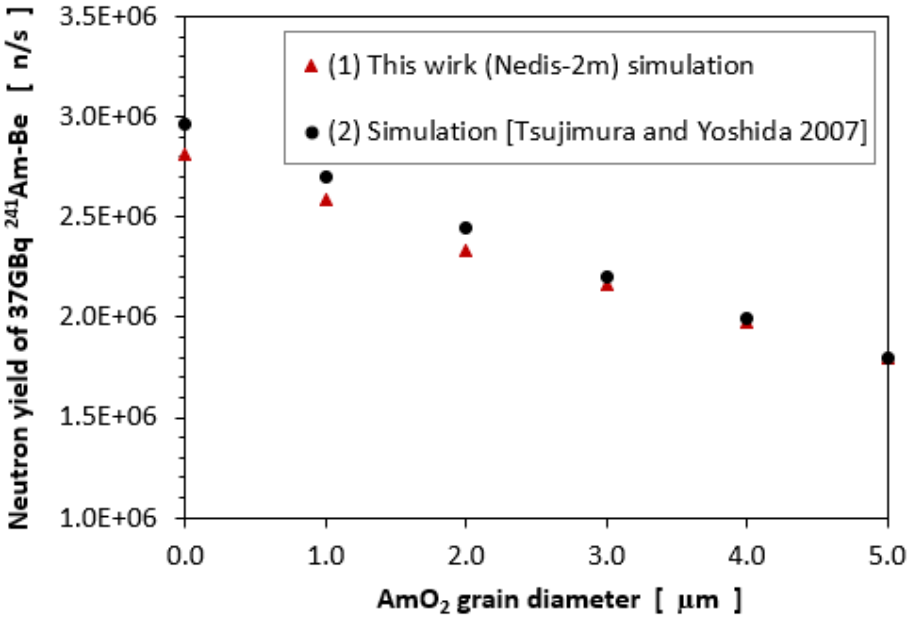

Figure 4.- Neutron yield of an ^{241}Am-Be neutron source (Amersham X.3 capsule) calculated as a function of AmO_2 grain diameter.

Table 2.- Comparison on neutron yield values for AmO_2-Be source of different grain sizes (Amersham X.3 capsule).

Grain diameter [μm]	**Nedis-2m calculations** (This work)	**Calculations reported in** (Tsujimura and Yoshida, 2007)	**Difference [%]**
0.0	2.82E+06	2.97E+06	5.10
1.0	2.59E+06	2.70E+06	4.23
2.0	2.33E+06	2.45E+06	4.67
3.0	2.16E+06	2.20E+06	1.97
4.0	1.98E+06	1.99E+06	0.64
5.0	1.80E+06	1.80E+06	0.03

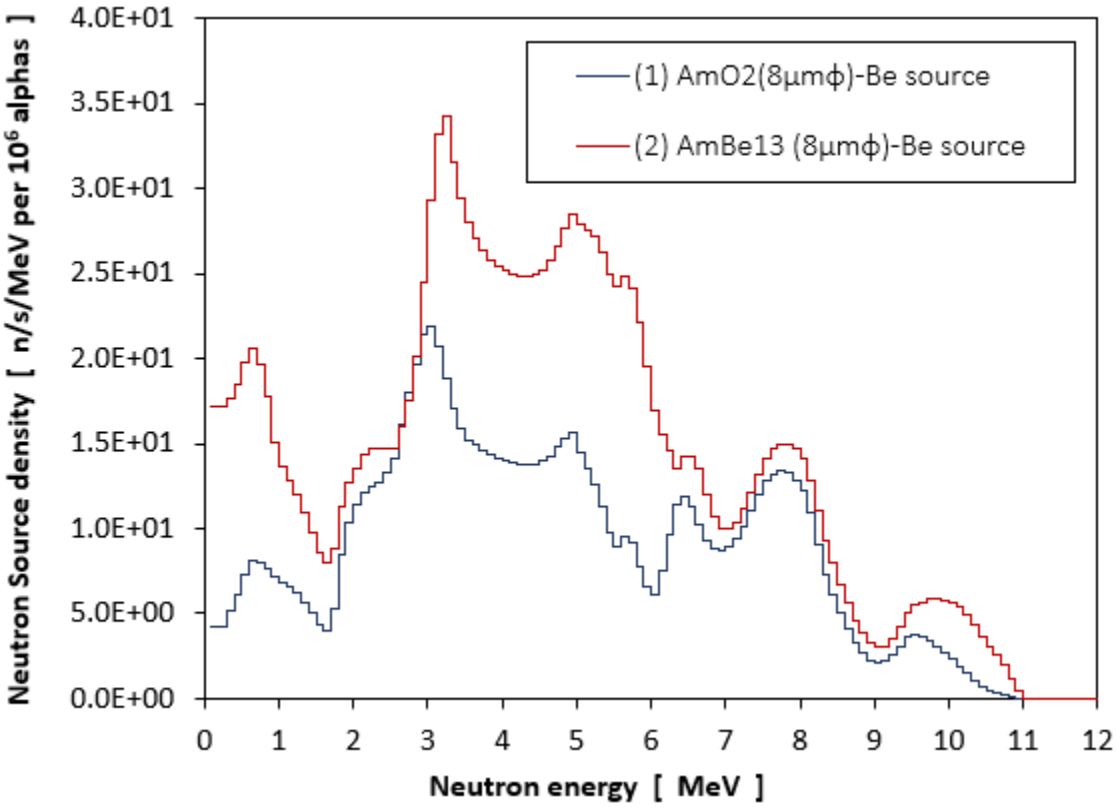

Figure 5.- A comparison on the calculated neutron spectra for AmO_2 (8 μmϕ) -Be and $AmBe_{13}$ (8 μm ϕ)-Be sources.

2.2.- Nedis-Serpent simulation of AmO_2-Be source

Nedis-2m program has been used to model the spontaneous fission and (α,n) reactions (Figs. 2-4). However, since neutrons generated in (α,n) reactions have high energies (E_{avg} = 4.69 MeV, E_{max} = 12 MeV), there is a probability for (n,2n) reaction on Be to occur, in addition to (n, fission), which can influence the neutron yield and energy distribution. The above-mentioned processes have been simulated by the hybrid use of Nedis-2m and Serpent 2.1.30 codes (ENDF-B/VII.0). The methodology of this approach has been described in (Ghal-Eh *et al*., 2019), which comprises two separate stages. At the first stage, the neutron energy spectrum is calculated within the capsule volume (Figs. 2-4). This neutron energy spectrum is used at the second stage as an initial condition for neutron transport simulation in order to calculate the neutron flux at the surface of AmO_2-Be capsule in the Serpent 2.1.30 program. The calculation in the Serpent 2.1.30 (ENDF-B/VII.0) has been performed on a high-performance cluster of Tomsk Polytechnic University, which consists of 6 nodes, each an Intel Xeon (E5-2697v3, 2.60GHz) with 64 GB RAM, 64-bit hardware.

The neutron flux, I_n (neutron current density on the surface) ($n/cm^2 \times s$), on the surface of the capsule has been tallied using a Surface Current Detector (det ds). In each calculation set, 1E9 neutron histories have been simulated in order to keep the errors well below 0.01% in the integral values, I_n, and also in the number of neutrons falling into the energy group i, $I_{ni}(E_i)$.

2.3.- Nedis-Serpent simulation of a neutron source assembly with complex internal heterogeneous structure

Radioisotopic neutron sources, especially Am-Be due to the long half-life of ^{241}Am and the neutrons and gamma-ray emission in non-working hours, require a strict protection. Such sources have severe radiation and chemical toxicities, therefore, they must be either disposed of or subject to complex chemical processing after the expiration of operation life.

This problem can be resolved in a neutron source of heterogeneous geometry where the source can be easily switched off by removing the Be layer, or by placing a sheet of appropriate material/size between the Be and Am (Ghal-Eh *et al*., 2019).

In this study, an AmO_2-Be source with heterogeneous assembly has been modeled following (Ghal-Eh *et al*., 2019). The overall dimensions of the source are identical to Amersham X.14 capsule, except for the active part consisting of 6 AmO_2 rods (diameter = 1.065 mm (hereinafter 1 mm), height = 5.05 cm) with a total weight of 0.476 × 6 = 2.86 g, instead of a fine-grained mixture of AmO_2 and Be. The rest of source assembly is so filled with beryllium (weighing 34.88 g) that the mass and density of the components (6 rods in Be) of the core are also identical to Amersham X.14 capsule. The calculated composition of AmO_2 rods is given in Table 4. The material compositions of stainless-steel shell are identical to those used by the manufacturer. In order to minimize the neutron absorption within the source shell, an aluminum capsule has been assumed, where the aluminum brand is SAV-1 (Lebedev *et al*., 2014) with the following composition (% wt.): Al (97.8); Mg (0.9); Si (1.17); Ni (0.03); Ti (0.01); Fe (0.05); Cu (0.01); Zn (0.03).

Table 4.- The material composition of AmO_2 rods.

Nuclide	Nuclide density [nuclides/(b·cm)]	Isotopic Abundance [%]	Nuclide atomic fraction	Nuclide mass fraction	Mass [g]
^{16}O	4.705E-02	99.757	6.651E-01	1.169E-01	0.056
^{17}O	1.686E-05	0.038	2.533E-04	4.452E-05	
^{18}O	8.591E-05	0.205	1.367E-03	2.402E-04	
^{241}Am	2.231E-02	94.613	3.154E-01	8.353E-01	0.420
^{242}Am	8.430E-04	3.596	1.199E-02	3.175E-02	
^{243}Am	4.189E-04	1.791	5.970E-03	1.581E-02	

As discussed earlier in Section 2.2, the calculation procedure consists of two stages. The neutron spectrum within AmO_2 rod is calculated at the first stage, before calculating the neutron spectrum at 300 μ (~ 10 × r_α) thick Be layer surrounding AmO_2 rod.

The yield and energy spectrum of neutrons in the AmO_2 rod have been calculated in Nedis-2m and is shown in Fig. 8 (see line (1)), whilst the same quantities have been calculated, but in a 300-μ Be layer, using MCNP 6.1 code (Pelowitz *et al*., 2014). The flux and energy distribution of alpha particles, $I_\alpha(E)$, emitted from the cylindrical lateral and flat end surfaces of the rod, which are considered as input data for MCNP 6.1, are listed in Table 5, which consists of 9 main lines corresponding to ^{241}Am, ^{242}Am and ^{243}Am isotopes.

Table 5.- The spectrum of alpha particles at the time of decay of isotopes Am.

$E_{\alpha i}$ [MeV]	y(i) [Bq × s]$^{-1}$	Yield [alpha particles/s]
5.14	3.22E-05	3.86E+06
5.18	1.79E-05	2.15E+06
5.21	4.81E-04	5.78E+07
5.23	1.23E-04	1.48E+07
5.28	9.77E-04	1.17E+08
5.37	2.22E-05	2.67E+06
5.43	1.94E-02	2.32E+09
5.44	1.28E-01	1.53E+10
5.49	8.51E-01	1.02E+11

The MCNP 6.1-calculated 600-group energy distribution of alpha particles, $I_\alpha(E)$, at the rod surface is illustrated in Fig. 6. The result is presented in the energy range of 0 to 6 MeV, with 0.01 MeV energy intervals. The errors in the calculated values of the integral flux, I_α, as well as the number of alpha particles that fall into the energy group i, $I_{\alpha i}$ (E), is less than 1% over the entire energy range. The spectrum of alpha particles I_α (E) (Fig. 6) have been folded into 22 groups (Fig. 7 and Table 6) to calculate the yield and spectrum of neutrons in 300-μ Be layer in Nedis-2m. The results are shown in Fig. 8, line (2).

At the second calculation stage, to calculate the neutron current density on the surface of the heterogeneous AmO_2-Be assembly, a 3D model has been created for the Serpent calculations. The 3D model consists of 12 computational zones, 6 zones with the spectrum

of type (1) (Fig. 8, Line 1) and 6 zones with the spectrum of type (2) (Fig. 8, Line 2). The data calculated with Serpent are illustrated in Fig. 8, Line 4.

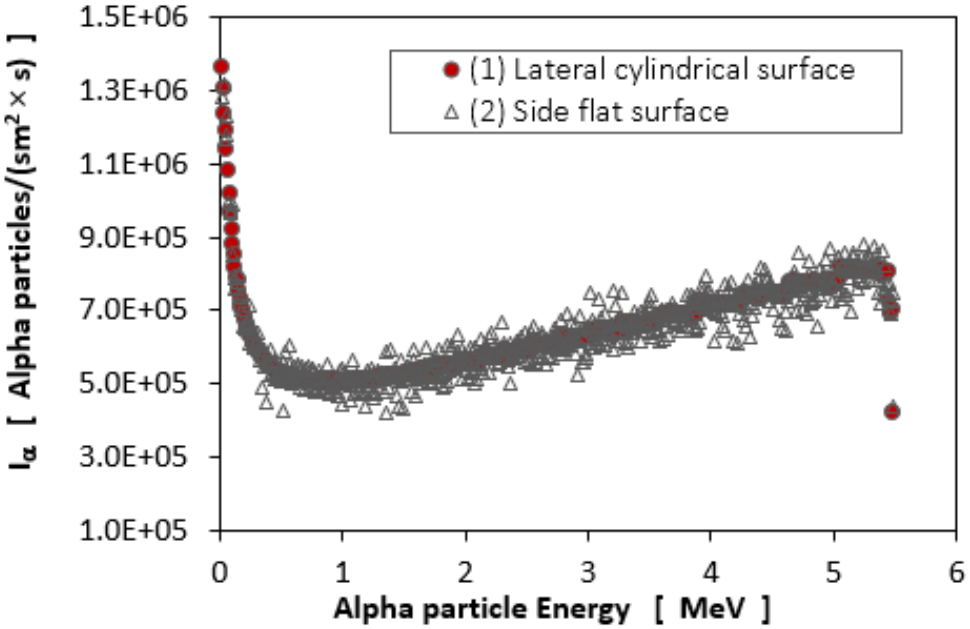

Figure 6.- Alpha particle energy spectrum at the surface of AmO_2 cylindrical rod.

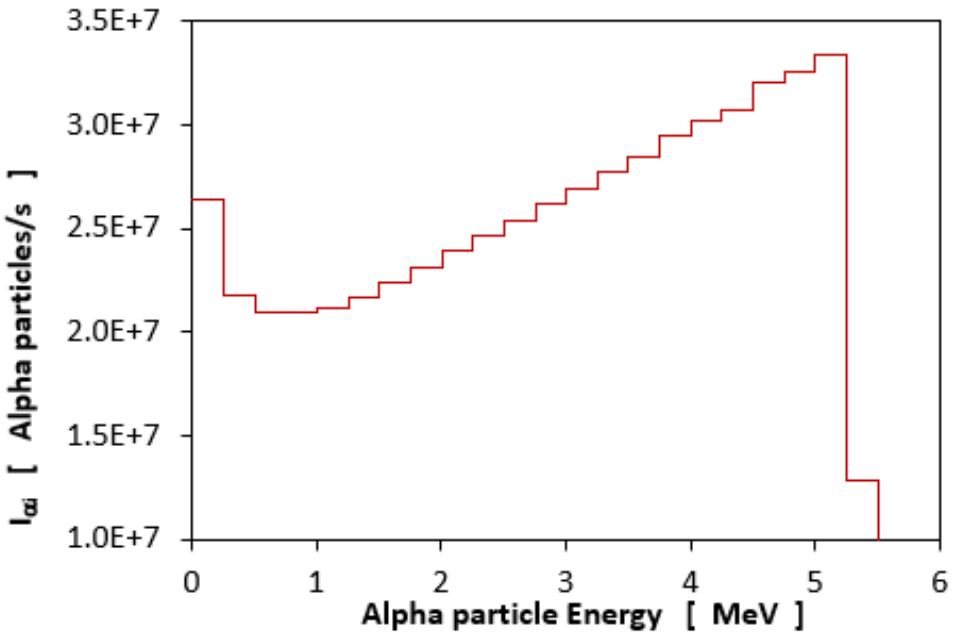

Figure 7.- 22-group alpha particle energy spectrum at a surface of AmO_2 cylindrical rod.

Table 6.- Radiation characteristics of the alpha particle calculated at the surface of AmO_2 rod.

№	E_{min} [MeV]	E_{max} [MeV]	$I_{\alpha i}$ [$\alpha/(sm^2 \times s)$]	$I_{\alpha i}$ [α/s]	Weight [$I_{\alpha i}/I_{\alpha}$]
0	0.005	0.255	1.66E+07	2.64E+07	4.69E-02
1	0.255	0.505	1.38E+07	2.18E+07	3.88E-02
2	0.505	0.755	1.32E+07	2.09E+07	3.72E-02
3	0.755	1.005	1.32E+07	2.09E+07	3.72E-02
4	1.005	1.255	1.34E+07	2.12E+07	3.77E-02
5	1.255	1.505	1.37E+07	2.17E+07	3.86E-02
6	1.505	1.755	1.41E+07	2.24E+07	3.99E-02
7	1.755	2.005	1.46E+07	2.31E+07	4.10E-02
8	2.005	2.255	1.50E+07	2.39E+07	4.24E-02
9	2.255	2.505	1.55E+07	2.46E+07	4.37E-02
10	2.505	2.755	1.60E+07	2.54E+07	4.51E-02
11	2.755	3.005	1.65E+07	2.62E+07	4.65E-02
12	3.005	3.255	1.70E+07	2.69E+07	4.78E-02
13	3.255	3.505	1.75E+07	2.77E+07	4.92E-02
14	3.505	3.755	1.79E+07	2.84E+07	5.06E-02
15	3.755	4.005	1.86E+07	2.95E+07	5.24E-02
16	4.005	4.255	1.90E+07	3.02E+07	5.36E-02
17	4.255	4.505	1.94E+07	3.07E+07	5.46E-02
18	4.505	4.755	2.02E+07	3.20E+07	5.69E-02
19	4.755	5.005	2.05E+07	3.25E+07	5.78E-02
20	5.005	5.255	2.11E+07	3.34E+07	5.94E-02
21	5.255	5.505	8.08E+06	1.28E+07	2.28E-02

The contribution of neutrons generated in (α,n) reactions on $^{17,18}O$ isotopes in AmO_2 rod is 9.53% (Y(AmO_2 (1 mm ϕ)) = 1.08×10^3 n/s) of the total number of neutrons Y(AmO_2 (1 mm ϕ) + Be) = 1.14×10^4 n/s (Fig. 8), whilst their contribution in the energy spectrum extends up to 6 MeV (Fig. 8, line (3)).

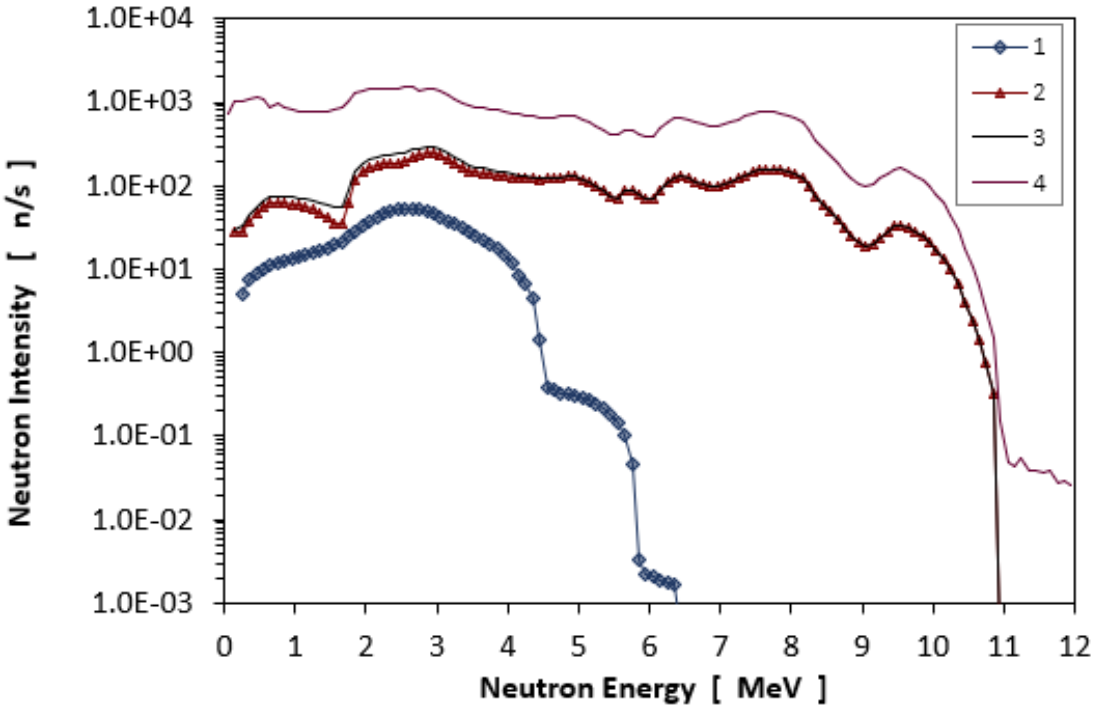

Figure 8.- The neutron energy spectrum calculated for a heterogeneous source (6 cylindrical AmO_2 rods in metallic Be): (1) neutron energy spectrum in an AmO_2 rod; (2) neutron energy spectrum in a 300 μm thick Be layer; (3) total neutron energy spectrum of the rod; (4) neutron energy spectrum at the surface of the capsule.

There is an additional neutron generation from (n,2n) reaction of about 5.88%, which can be seen as a high-energy tail in the energy range of 11 to 12 MeV in Fig. 8 (line (4)).

Note should be taken that the iterative nature of MCNP 6.1 in modeling $I_\alpha(E)$ spectrum may be excluded from the calculations by using Nedis-2m code instead, however, Nedis-2m is unable to create cylindrical heterogeneous structures.

In order to obtain a satisfactory result, one may replace the cylindrical geometry with an equivalent planar one. This assumption seems to be acceptable because the condition of $r_{rod} >> r_\alpha$ is still valid, which is the reason for the similarity of the calculated results shown in Fig. 6 to the alpha particles emitted from a cylindrical (line (1)) and flat (line (2)) surfaces. A planar AmO_2 source is taken with a thickness of 263 μm at a given density of 10.6 g/cm^3

and a cylindrical surface area of 1.70 cm^2, corresponding to an Am mass of 0.420 g (Table 3). The calculated neutron yield for such a source is Y(AmO_2 (263 μm) + Be) = 1.31 × 10^4 n/s, which is in a promising agreement with the previously-calculated value for the cylindrical rod, Y(AmO_2 (1 mm ϕ) + Be) = 1.14 × 10^4 n/s (Note: The result is overestimated by 27.4% compared to a more accurate modeling).

3. RESULTS AND DISCUSSION

The neutron energy spectra of encapsulated neutron sources of Amersham X.3 and X.14, performed in Nedis-2m program code are shown in Figs. 2-4. These spectra exhibit good agreement (no more than 5%) with both the calculations (Tsujimura and Yoshida, 2007) and measurements (Kluge and Weise, 1982; Marsh *et al*., 1995), as summarized in Table 7.

Table 7.- Neutron yields of an AmO_2-Be source obtained using different codes and measurements.

Case number	Capsule type	Simulation code	Active part of Am-Be source	Source material composition	Neutron yield [n/s]
Z1	X.14	SOURCES-4C	Homogeneous AmO_2-Be source	AmO_2 2.86 g Be 34.88 g	2.37(7)
Z2		Nedis-2m			2.31(7)
Z3		Nedis-2m	AmO_2 (8μmϕ)-Be source		1.20(7)
Z4		Nedis-2m	$AmBe_{13}$ (8μmϕ)-Be source	$AmBe_{13}$ 3.15 g Be 34.63 g	1.78(7)
Z5	X.3	Nedis-2m	AmO_2 (2μmϕ)-Be Source	AmO_2 0.37 g Be 4.6 g	2.33(6) (This work) 2.45(6) (Tsujimura and Yoshida, 2007) 2.42(6) (Marsh *et al*., 1995)

The decrease in the integral neutron yield (Table 7, Cases Z2, Z3, and Z5) is believed to be caused by the slowing down and spectrum softening of very short-range alpha particles (Fig. 6). Moreover, some alpha particles remain inside the grain and hardly participate in neutron production via (α,n) reaction to ^{9}Be. It is seen that the contribution of neutrons generated in (α,n) reactions on ^{17,18}O inside AmO_2 grains (for the grain size of 8 μm ϕ) does not exceed 0.05% of the total number of neutrons.

Besides, the use of stable crystals of $AmBe_{13}$ intermetallic compounds (Table 7, Case Z4) does not considerably change the situation (*i.e.*, the increase in neutron yield is less than 50%). The calculated neutron spectrum, $N_n(E_n)$ within the volume of X.14 capsule and on its entire surface, $I_n(E_n)$, is presented in Fig. 9 and Table 8.

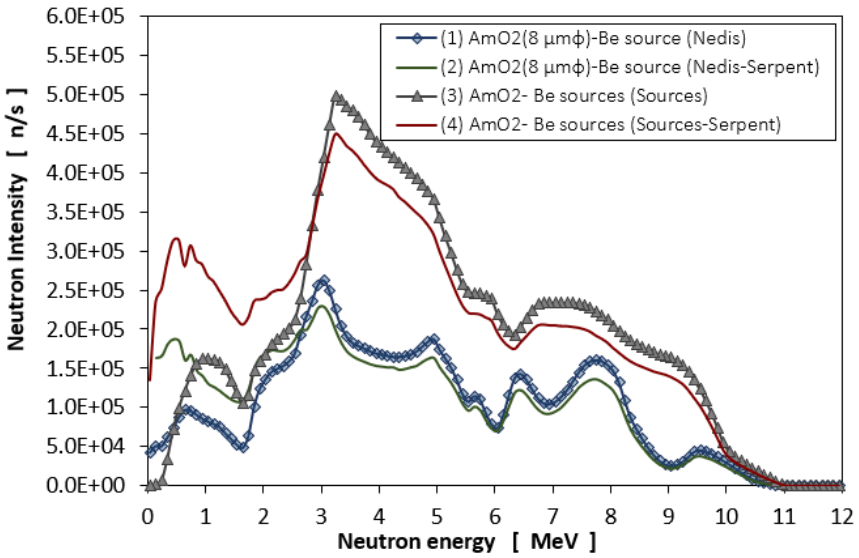

Figure 9.- Energy spectrum of neutrons produced inside the volume (lines 1 and 3) and at the surface of the capsule (lines 2 and 4).

It can be seen from the neutron energy spectra of Fig. 9 (line (2)) that the characteristic peaks of the Am-Be source, $E_{\alpha i}$ = 3.1, 4.8, 6.6, 7.7, and 9.8 MeV, satisfactorily coincide with the measurements data published in (Haas and McCarthy, 1967; Van Der Zwan, 1968; Notarrigo *et al.*, 1969; Lorch, 1973; Kluge and Weise, 1982; Marsh *et al.*, 1995)). However, the shift of initial spectra (lines (1) and (3)) to lower energies may be attributed

to neutron slowing down as a result of elastic and inelastic scatterings on the constituent nuclei of both the source core and the shell.

The high-energy neutron spectrum (Fig. 9, lines (1) and (3)) generated in (α,n) reactions most probably initiates the threshold reactions (n,fission) and (n,2n) (See Table 8). Note that for Cases Z6 and Z7, more than 95 % of the neutrons are generated from (α,n) and the rest from threshold reactions.

Table 8.- A comparison on the results obtained for Am-Be sources calculated with different hybrid codes.

Case number	**Code**	**Am-Be core type**	**Source material composition**	**I_n [n/s]**	**Relative difference [%]**
Z6	SOURCES4C-Serpent2.1.30	Homogeneous AmO_2-Be	AmO_2 2.86g	2.47E+07	[Y(Z6) – Y(Z1)]/ Y(Z1) = 4.22
Z7	Nedis2m-Serpent2.1.30	AmO_2 (8μmϕ) - Be	Be 34.88 g	1.23E+07	[Y(Z7) – Y(Z3)]/ Y(Z3) = 3.5

The results obtained for the heterogeneous AmO_2 (1 mm ϕ)-Be assembly (see Table 9) are similar to the previous ones (see Tables 7 and 8), but not identical. Since the neutron sources are actually the cylindrical rods and not spread throughout the capsule, the (α,n)-generated neutrons are most probably travel within Be.

Since Be is an efficient neutron moderator, it results in a decrease in neutron yield (see Table 9, Case Z8) as well as softening the energy spectrum (see Fig. 10, line 1).

The results in Table 9 confirm that the additional neutron yield is mainly attributed to (n,2n) reaction.

In addition, the use of SAV-1 aluminum alloy as a capsule shell does not result in a significant decrease in neutron flux, most likely due to the relatively small size of the capsule and high average energy of generated neutrons.

Table 9.- Neutron components of the radiation characteristics calculated for various types of Am-Be source.

Case number	Type of Am-Be core	Material composition	Neutron flux I_n [n/s]		Neutron yield [n/s]		
			Capsule shell material		Parameter	Capsule shell material	
			Steel	Aluminum		Steel	Aluminum
Z7	AmO_2(8μmϕ)-Be	AmO_2 2.86g Be 34.88g	1.23(7)	-	Neutron Yield (Case Z3)	1.20(7)	
Z8	6 AmO_2(1 mmϕ)-Be	AmO_2 2.86 g Be 34.88g	7.20(4)	7.25(4)	Neutron Yield (1 rod)	1.14(4)	1.14(4)
					Weight (particles /src)	1.14(-5)	1.14(-5)
					Neutron origin (reaction (fission, n))	9.65(1) (0.85 %)	1.59(2) (1.39 %)
					Neutron origin (reaction (n,xn))	6.70(2) (5.88 %)	6.54(2) (5.73 %)
					Lost neutrons (reaction (n, capture))	1.34(2) (1.17 %)	1.26(2) (1.11 %)

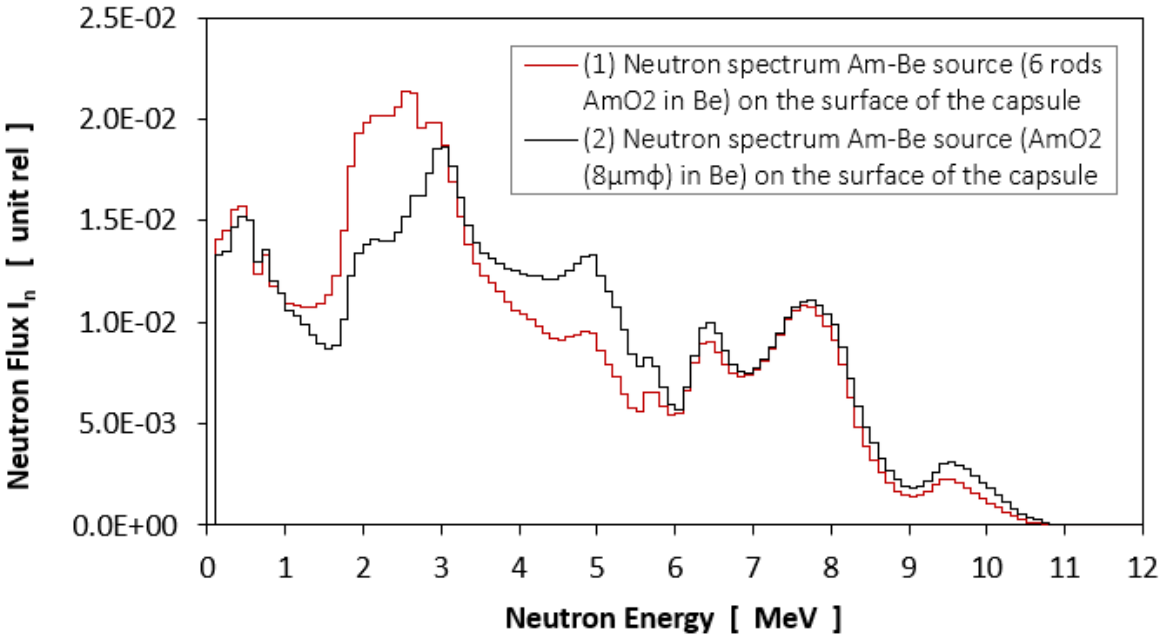

Figure 10.- Comparison of normalized neutron spectra calculated for heterogeneous (6 cylindrical AmO_2 rods (1 mm ϕ) in metallic Be) and homogeneous (spherical AmO_2 grains (8 μm ϕ) in metallic Be) sources.

Fig. 11 shows a comparison between the neutron spectrum at the surface of an Am-Be assembly and the neutron spectrum generated by DT reactions in a long magnetic trap with a high-temperature plasma (Arzhannikov *et al*., 2019).

The comparison confirms that the irradiation facility consisting a number of heterogeneous Am-Be assemblies can generate neutrons with a very similar spectrum to that of DT neutrons. Such an irradiation facility, if it can generate a neutron flux density of ~ 10^{12} n/cm^2 - s, is a unique source for studying the properties of materials and equipment used in thermonuclear energy systems.

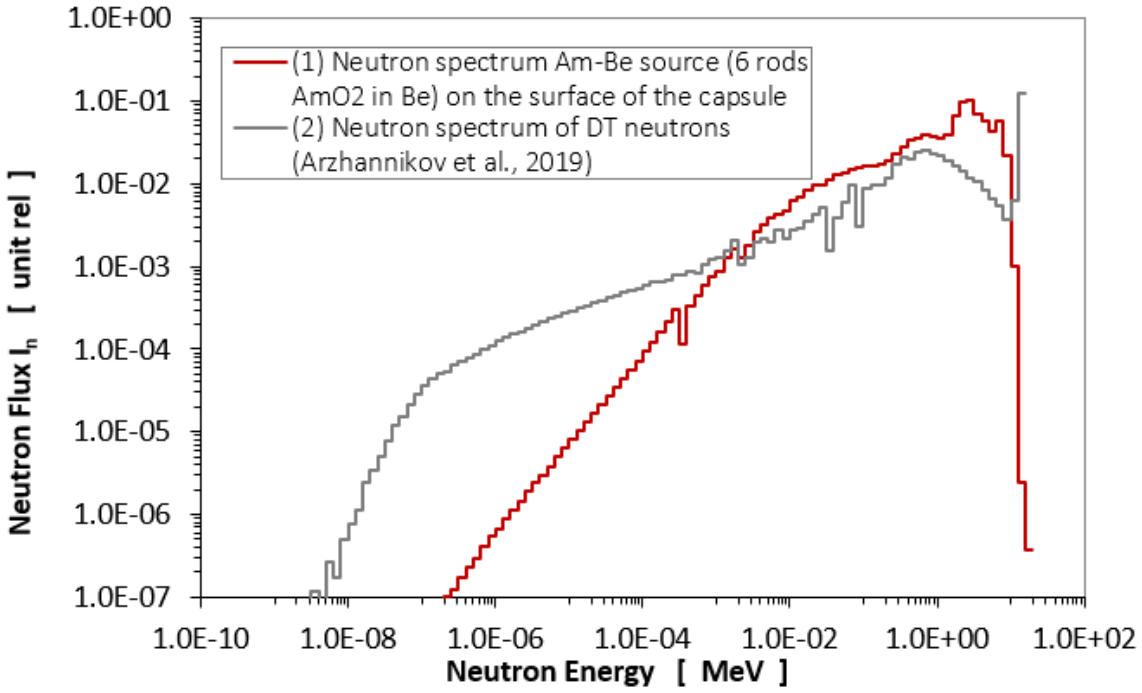

Figure 11.- Comparison of normalized neutron spectra calculated for the heterogeneous AmO_2 (6 cylindrical AmO_2 rods (1 mm ϕ) in metallic Be) and DT neutron sources.

4.- CONCLUSIONS

In this study, a hybrid use of Nedis-2m and Serpent 2.1.30 codes in predicting the radiation characteristics of Am-Be neutron source of a complex heterogeneous structure has been presented. In addition, the neutronic features of an encapsulated Am-Be neutron source, with a fine-grained mixture of AmO_2 and Be crystals as a core, has been investigated. Likewise, the variations of the yield and energy spectrum of Am-Be source neutron against the grain size of crystals have been demonstrated. The possibility of increasing the neutron yield has been considered using stable $AmBe_{13}$ crystals. Both an analytical model and verified calculation codes have been performed using Nedis-2m and Serpent 2.1.30, to introduce a methodology for calculating the yield and energy spectrum of a neutron source with heterogeneous active part of AmO_2 rods embedded in Be. By a comparative analysis, it was shown that an irradiation facility assembled from the nth number of heterogeneous Am-Be sources can produce neutrons with a spectrum similar to DT neutron generator

(Arzhannikov *et al*., 2019). Such an irradiation facility, with capability of producing a neutron flux density of ~ 10^{12} n/cm^2 - s can benefit the study of the properties of materials and equipment used in thermonuclear energy. The neutron yield in such a setup can basically increase by adding the number of AmO_2 rods in the beryllium matrix, yet, the use of hollow AmO_2 rods almost doubles the neutron yield.

Acknowledgements

This work was carried out as part of an initiative project to design and construct a unique irradiation facility to study the properties of materials and equipment operating in the epithermal neutron field, which was supported by the RFBR (Project №. 19-29-02005\19).

REFERENCES

Amersham/Searle. (1976). *Neutron sources ^{241}Am-Be and ^{252}Cf*. Technical Bulletin: 76-77.

Arzhannikov AV; Shamanin IV; Bedenko SV; Prikhodko VV; Sinitsky SL; Shmakov VM; Knyshev VV; Lutsik IO. (2019). *Hybrid thorium energy producing subcritical stand with a fusion neutron source based on a magnetic trap.* Izvestiya vuzov. Yadernaya Energetika **2**: 43-54. (in Russian).

Asamoah M; Nyarko BJB, Fletcher JJ; Sogbadji RBM; Yamoah S, Agbemava SE; Mensimah E. (2011). *Neutron flux distribution in the irradiation channels of Am-Be neutron source irradiation facility*. Annals of Nuclear Energy **38**: 1219-1224.

Bair JK; Gomez del Campo J. (1979). *Neutron Yields from Alpha-Particle Borbardment*. Nuclear Science and Engineering **71**: 18-28.

Balaghi S; Ghal-Eh N; Mohammadi A; Vega-Carrillo HR. (2018*). A neutron scattering soil moisture measurement system with a linear response*. Applied Radiation and Isotopes **142**: 167-172.

Bedenko SV; Ghal-Eh N; Lutsik IO; Shamanin IV. (2019). *A fuel for generation IV nuclear energy system: Isotopic composition and radiation characteristics.* Applied Radiation and Isotopes **147**: 189-196.

Croft S. (1989). *The use of neutron intensity calibrated ^{9}Be(α,n) sources as 4438 keV gamma-ray reference standards.* Nuclear Instruments and Methods in Physics Research A: Accelerators, Spectrometers, Detectors and Associated Equipment **281**: 103-116.

Didi A; Dadouch A; Jaï O; Tajmouati J; Bekkouri HEl. (2016). *Neutron activation analysis: Modelling studies to improve the neutron flux of Americium-Beryllium source*. Nuclear Engineering and Technology **49:** 787-791.

Dim OU; Aghara SK. (2019). *Computation of the neutron multiplicity moments for research reactor fuels using MCNP6 and SOURCES4C.* International journal of energetic research **2019**: 1-12.

Fernandes AC; Kling A; Vlaskin GN. (2017). *Comparison of thick-target (alpha,n) yield calculation codes.* EPJ Web of Conferences **153**: 07021.

Geiger KW; Van Der Zwan L. (1975). *Radioactive neutron source spectra from ^{9}Be(α, n) cross section data.* Nuclear Instruments and Methods **131**: 315-321.

Ghal-Eh N; Rahmani F; Bedenko SV. (2019). *Conceptual design for a new heterogeneous ^{241}Am-^{9}Be neutron source assembly using SOURCES4C-MCNPX hybrid simulations.* Applied Radiation and Isotopes **153**: 108811.

Griesheimer DP; Pavlou AT; Thompson JT; Holmes JC; Zerkle ML; Caro E; Joo H. (2017). *In-line (α,n) source sampling methodology for monte carlo radiation transport simulations*. Nuclear Engineering and Technology **49**: 1199-1210.

Haas FX; McCarthy JT. (1967). *A stilbene fast neutron spectrometer for the study of the neutron spectrum of a Pu-Be source.* Nuclear Instruments and Methods **50**: 340-342.

Heaton R; Lee H; Skensved P; Robertson BC. (1989). *Neutron Production from Thick-Target (α,n) Reactions*. Nuclear Instruments and Methods in Physics Research Section A: Accelerators, Spectrometers, Detectors and Associated Equipment **276**: 529-538.

Hermann OW; Westfall RM. (1995). *ORIGEN-S: SCALE System Module to Calculate Fuel Depletion, Actinide Transmutation, Fission Product Buildup and Decay, and Associated Radiation Source Terms*. Vol. II, Sect. F7 of SCALE: A Modular Code System for Performing Standardized Computer Analyses for Licensing Evaluation NUREG/CR-0200.

International Organization for Standardization. Reference neutron radiations-part 1, characteristics and methods of production. ISO 8529-1 (Geneva: ISO) (2001).

Kluge H., Weise K. (1982). *The neutron energy spectrum of a ^{241}Am-Be (Alpha,n) source and resulting mean fluence to dose equivalent conversion factors*. Radiation Protection Dosimetry **2**: 85-93.

Lebedev VM; Lebedev VT; Orlov SP; Margolin BZ; Morozov AM. (2014). Issledovaniye nanorazmernoy struktury, s pomoshch'yu neytronov s vysokim urovnem rasseyaniya, metodom malouglovogo rasseyaniya neytronov. Fizika tverdogo tela 56: 11-23. (in Russia).

Lebreton L; Zimbal A; Thomas D. (2007). *Experimental comparison of ^{241}Am-Be Neutron fluence energy distributions*. Radiation Protection Dosimetry **126**: 3-7.

Leniau B; Wilson JN. (2014). *A new spent fuel source characterization code CHARS and its application to the shielding of the thorium cycle.* Progress in Nuclear Science and Technology **4**: 134-137.

Leppänen J; Pusa M; Viitanen T; Valtavirta V; Kaltiaisenaho T. (2015). *The Serpent Monte Carlo code: Status, development and applications in 2013.* Annals of Nuclear Energy **88**: 142-150.

Liu Z; Chen J, Zhu P, Li Y, Zhang G. (2007). *The 4.438 MeV gamma to neutron ratio for the Am-Be neutron source.* Applied Radiation and Isotopes **65**: 1318-1321.

Lorch EA. (1973). *Neutron Spectra of ^{214}Am/B, ^{241}Am/Be, ^{241}Am/F, ^{242}Cm/Be, ^{238}Pu/^{13}C and ^{252}Cf isotopic neutron sources.* The International Journal of Applied Radiation and Isotopes **24**: 585-591.

Marsh JW; Thomas DJ; Burke M. (1995). *High resolution measurements of neutron energy spectra from Am-Be and Am-B neutron sources.* Nuclear Instruments and Methods in Physics Research Section A: Accelerators, Spectrometers, Detectors and Associated Equipment **336**: 340-348.

Mei DM; Zhang C.; Hime A. (2009). *Evaluation of (α,n) induced neutrons as a background for dark matter experiments*. Nuclear Instruments and Methods in Physics Research Section A: Accelerators, Spectrometers, Detectors and Associated Equipment **606**: 651-660.

Murata T; Shibata K. (2002). *Evaluation of the (α,n) Reaction Nuclear Data for Light Nuclei*. Journal of Nuclear Science and Technology **39:** 76-79.

Murata T; Matsunobu H; Shibata K. (2006). *Evaluation of the (α,xn) Reaction Data for JENDL/AN-2005.* **Report JAEA-Research 2006-052** Japan Atomic Energy Research Institute.

Notarrigo S; Porto F; Rubbino A; Sambataro S. (1969). *Experimental and calculated energy spectra of Am-Be and Pu-Be neutron sources*. Nuclear Physics A **125:** 28-32.

Pelowitz D; Fallgren A; McMath G. (2014). *MCNP6 User's Manual Code Version 6.1.1 Beta*. **Report LA-CP-14-00745** Los Alamos National Laboratory. New Mexico.

Plevaka MN; Bedenko SV; Gubaidulin IM; Knyshev VV. (2015). *Neutron-physical studies of dry storage systems of promising fuel compositions*. Bulletin of the Lebedev Physics Institute **42:** 240-243.

Reilly D; Ensslin N; Smith H. (1991). *Passive Nondestructive Assay of Nuclear Materials*. **Report NUREG/CR-5550** Los Alamos National Laboratory. USA.

Tsujimura N; Yoshida T. (2007). *Calculation of Anisotropy Factors for ^{241}Am-Be Neutron Sources*. Radioisotopes **56**: 497-508.

Van Der Zwan L. (1968). *Calculated neutron spectra from ^{9}Be(α, n) sources*. Canadian Journal of Physics **46**: 1527-1536.

Vega-Carrillo HR; Manzanares; Becerra-Ferreiro AM; Carrillo-Nuñez A. (2002). *Neutron and gamma-ray spectra of ^{239}PuBe and ^{241}AmBe*. Applied Radiation and Isotopes **57**: 167-170.

Vega-Carrillo HR; Martinez-Ovalle SA. (2016). *Few groups neutron spectra, and dosimetric features, of isotopic neutron sources*. Applied Radiation and Isotopes **117**: 42-50.

Vitorelli JC; Silva AX; Crispim VR; Fonseca ES; Pereira WW. (2005). *Monte Carlo simulation of response function for a NaI(Tl) detector for gamma rays from ^{241}Am/Be source.* Applied Radiation and Isotopes **62**: 619-622.

Vlaskin G; Khomiakov Y. (2017). *Calculation of Neutron Production Rates and Spectra from Compounds of Actinides and Light Elements*. EPJ Web of Conferences **153**: 07033.

Vlaskin GN; Khomyakov YS; Bulanenko VI. (2015). *Neutron Yield of the Reaction (α, n) on Thick Targets Comprised of Light Elements*. Atomic Energy **117**: 357.

Vlaskin GN. (2006). *NEDIS2.0 Code for Calculating the Neutron Yield and Spectra from (α, n) Reactions on the Nuclei of Light Elements and Owing to Spontaneous Fission*. **Report VNIINM 06-1** Bochvar High-Technology Research Institute of Inorganic Materials. Russia.

West D; Sherwood AC. (1982). *Mesurments of Thick-Target (α,n) Yields from Light Elements*. Annals of Nuclear Energy **9**: 551-577.

Wilson WB; Perry RT; Stewart JE; England TR., Arthur ED; Madland DG. (1984). *Development of SOURCES Code and Data Library for the Calculation of (alpha,n), Delayed Neutrons, (gamma,n) and Spontaneous Fission Decay Neutron Sources and Spectra*. **Report BNL-NCS-34291** Brookhaven National Laboratory. USA.

Wilson WB; Perry RT; Charlton WS. (2002). *SOURCES 4C: A Code for Calculating (α,n), Spontaneous Fission, and Delayed Neutron Source and Spectra*. **Report LA-UR-02-1839** Los Alamos National Laboratory. USA.

Yücel H; Budak MG; Karadag M; Yüksel AÖ. (2014). *Characterization of neutron flux spectra in the irradiation sites of a 37GBq ^{241}Am-Be isotopic source.* Nuclear Instruments and Methods in Physics Research Section B: Beam Interactions with Materials and Atoms **338**: 139-144.